ACCRETION DISKS WITH A LARGE SCALE MAGNETIC FIELD AROUND BLACK HOLES.

G.S. Bisnovatyi-Kogan

IKI RAN

In collaboration with R. Lovelace, A. Klepnev.

Vulcano Workshop
31 May 2012

Quasars and AGN contain supermassive black holes

About 10 HMXR - stellar mass black holes in the Galaxy: microquasars.

Jets are observed in objects with black holes:
collimated ejection from accretion disks.

Jet in M87:

radio, 14GHz, **VLA**, 0.2”

HST (F814W)

Chandra image, 0.2”, 0.2-8 keV

Adaptively smoothed **Chandra** image

From

Marshall et al. (2001)

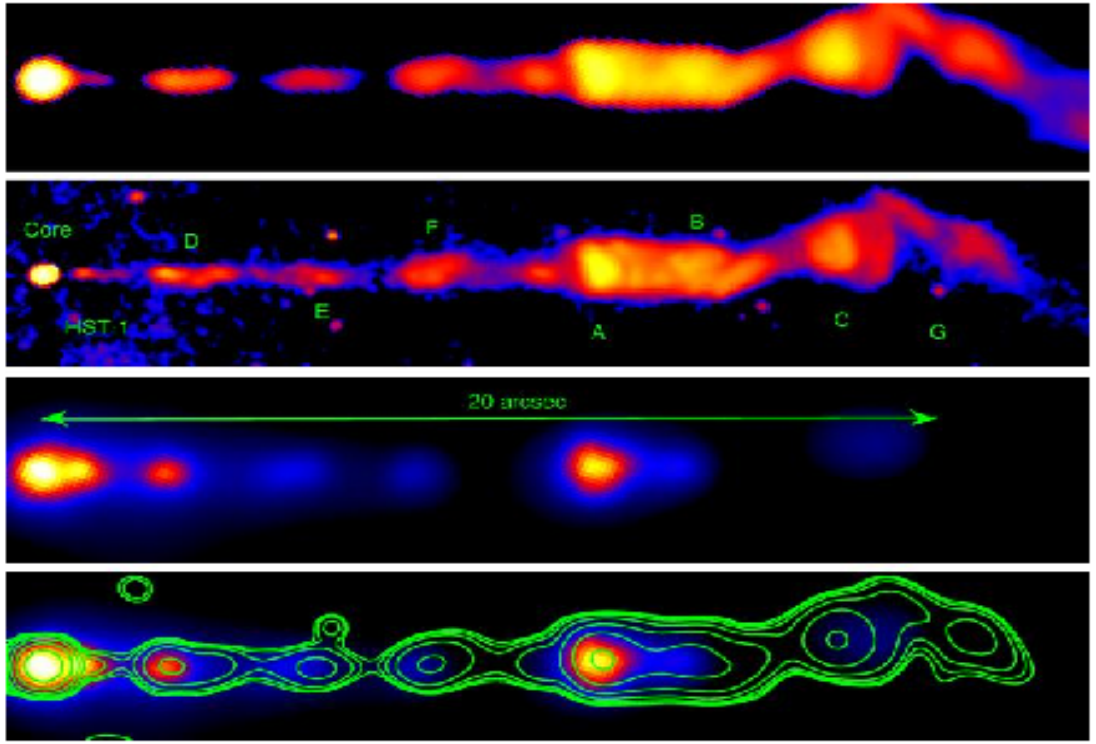

Fig. 1.— Images of the jet in M 87 in three different bands, rotated to be horizontal, and an overlay of optical contours over the X-ray image. *Top:* Image at 14.435 GHz using the VLA. The spatial resolution is about 0.2″. *Second panel:* The *Hubble* Space Telescope Planetary Camera image in the F814W filter from Perlman et al. (2001a). The brightest knots are labelled according to the nomenclature used by Perlman et al. (2001a) and others. *Third panel:* Adaptively smoothed *Chandra* image of the X-ray emission from the jet of M 87 in 0.20″ pixels. The X-ray and optical images have been registered to each other to about 0.05″ using the position of the core. *Fourth panel:* Smoothed *Chandra* image overlaid with contours of a Gaussian smoothed version of the HST image, designed to match the *Chandra* point response function. The X-ray and optical images have been registered to each other to about 0.05″ using the position of the core. The HST and VLA images are displayed using a logarithmic stretch to bring out faint features while the X-ray image scaling is linear.

3C 273

Left:

MERLIN, 1.647 GHz.

Middle:

HST(F622W), 6170A.

Right:

Chandra, 0.1 “

Marshall et al. (2000)

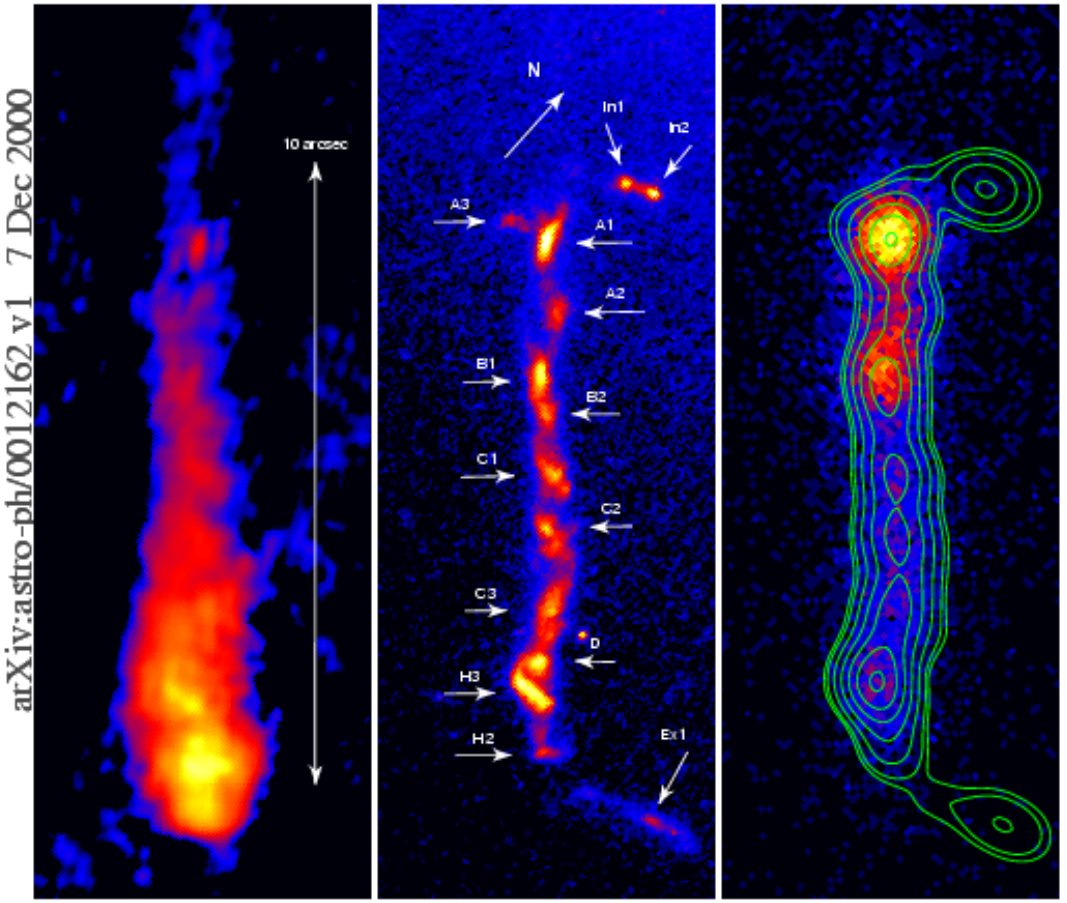

Jet in radiogalaxy

IC 4296 at 20 cm with 3.2" resolution.

10" is about 2 kps.

VLA, Killeen et al. (1986)

Total extent is about

400 kpc

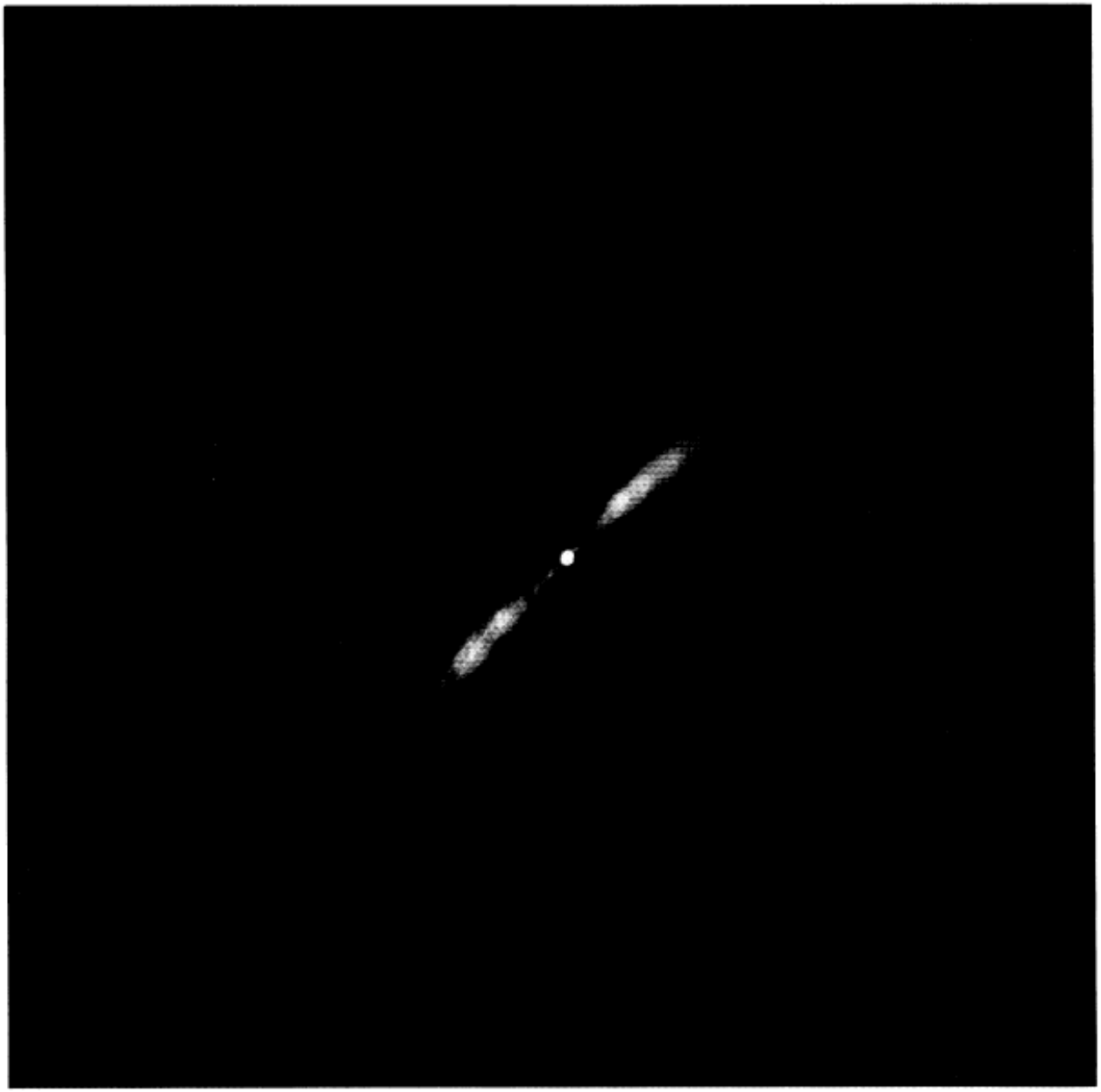

FIG. 11.—Radiograph of the jets at 20 cm with 3".2 resolution

KILLEEN (*see* page 311)

Microquasar

GRS 1915+105

Jet ejection

MERLIN 5GHz

Fender (1999)

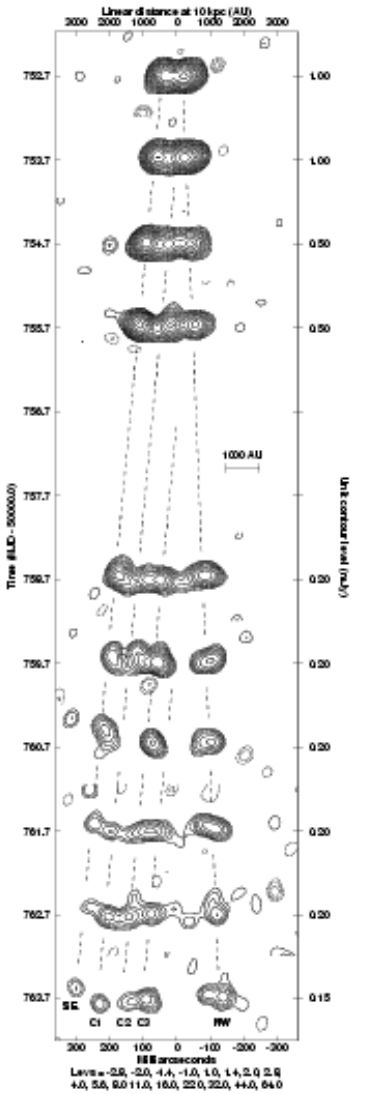

Fig. 2. A sequence of ten epochs of radio imaging of relativistic ejections from the black hole candidate X-ray binary GRS 1915+105 using MERLIN at 5 GHz. The figure has been rotated by 52 degrees to form the montage. Contour levels increase in factors of $\sqrt{2}$ from the unit contour level indicated at the right hand side of each image. Components SE, C1, C2 & C3 are approaching with a mean proper motion of 23.6 ± 0.5 mas d^{-1}. Component NW is receding with a mean proper motion of 10.0 ± 0.5 mas d^{-1} and corresponds to the same ejection event which produced approaching component SE. For an estimated distance to the source of 11 kpc the approaching components have an apparent transverse velocity of $1.5c$. Assuming an intrinsically symmetric ejection and the standard model for apparent superluminal motions, we derive an intrinsic bulk velocity for the ejecta of $0.98^{+0.02}_{-0.09}c$ at an angle to the line of sight of 66 ± 2 degrees (at 11 kpc). The ejections occurred after a 20-day 'plateau' during which the X-ray emission was hard and stable and the radio had an inverted spectrum. The first two ejections were punctuated by four days of rapid radio oscillations, indicative of an unstable inner accretion disc being repeatedly ejected [14,38,34,8,16]. The apparent curvature of the jet is probably real, although the cause of the bending is uncertain. A detailed presentation and discussion of these results may be found in [18].

THE ACCRETION OF MATTER BY A COLLAPSING STAR IN THE PRESENCE OF A MAGNETIC FIELD

G. S. BISNOVATYI-KOGAN and A. A. RUZMAIKIN
Institute of Applied Mathematics, U.S.S.R. Academy of Sciences, Moscow, U.S.S.R.

(Received June 27, 1973)

Astrophysics and Space Science **28** (1974) 45–59.

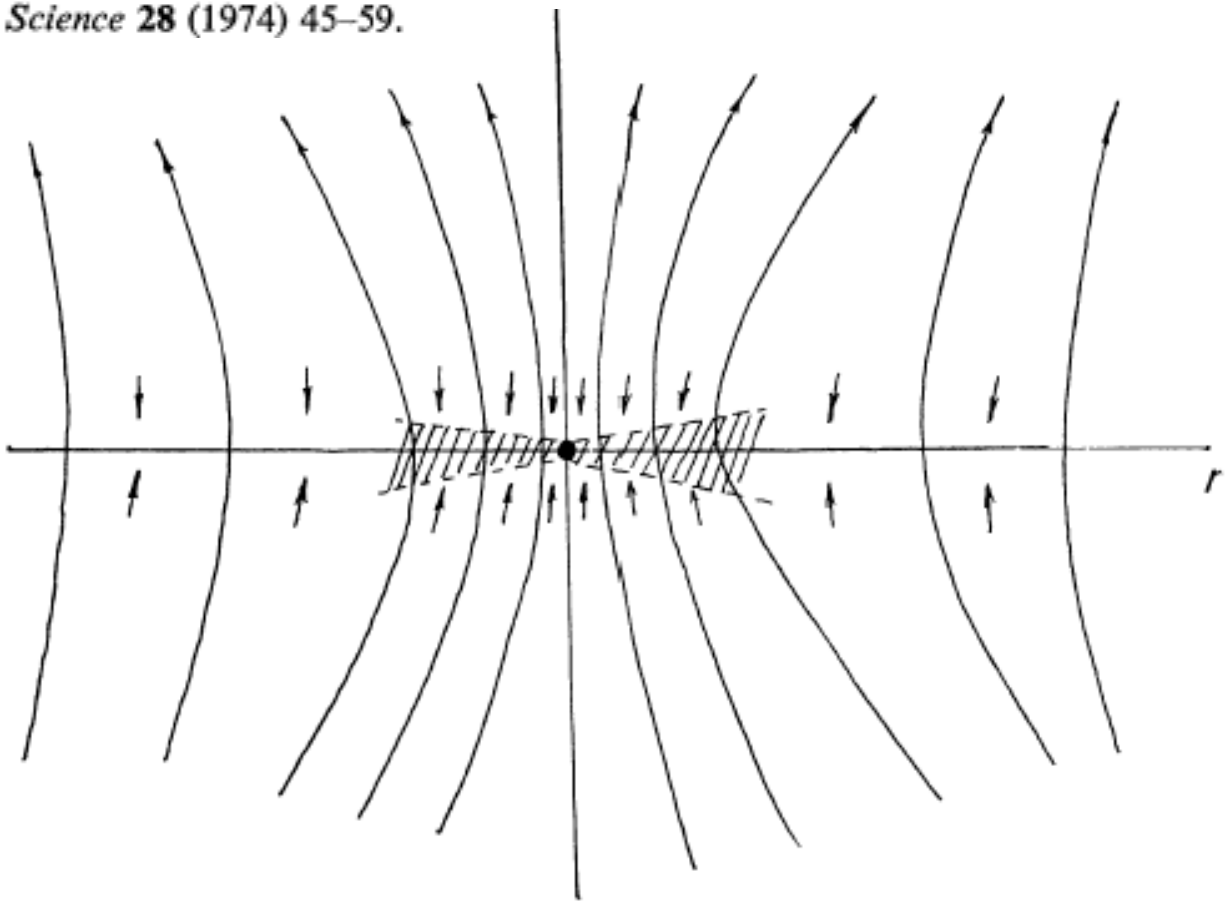

Fig. 1. A qualitative picture of the accretion of matter on to a c.s. with a frozen, regular magnetic field. Arrows indicate the direction of motion of the matter. The magnetic field far from the star lies in the direction of the z-axis and its sense is indicated by arrows on the lines of force. The infalling matter forms a disk in the plane $\theta = \pi/2$, which slowly settles to the star. In the flow region $E_B \sim E_{\text{kin}}$, and rotation is entirely absent.

THE ACCRETION OF MATTER BY A COLLAPSING STAR IN THE PRESENCE OF A MAGNETIC FIELD. II. SELFCONSISTENT STATIONARY PICTURE

G. S. BISNOVATYI-KOGAN
Space Research Institute, U.S.S.R. Academy of Science, Moscow, U.S.S.R.
and
A. A. RUZMAIKIN
Institute of Applied Mathematics, U.S.S.R. Academy of Science, Moscow, U.S.S.R.

(Received 26 August, 1975)

Astrophysics and Space Science **42** (1976) 401–424.

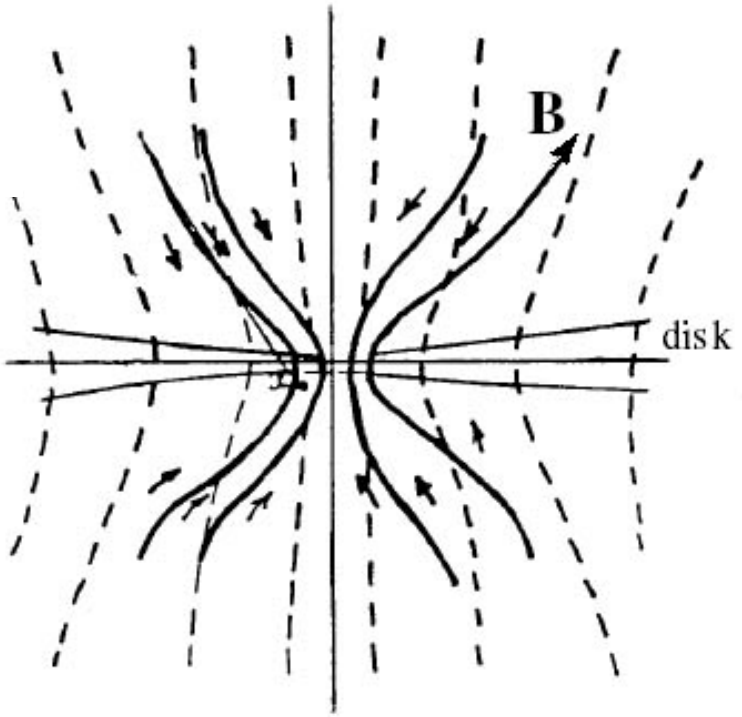

Sketch of the magnetic field threading an accretion disk.
Shown increase of the field owing to flux freezing in the accreting disk matter

At presence of large-scale magnetic field the efficiency of accretion is alvays large (0.3-0.5) of the rest mass energyflux

Accretion disk around BH with large scale magnetic field (non-rotating disk)

The Basic Equations for the Stationary Disc Structure in the Plane $\theta = \pi/2$

$$\frac{GM\Sigma}{r^2} \simeq \frac{1}{c} B_\theta I_\varphi \simeq \frac{2\pi}{c^2} I_\varphi^2, \qquad B_\theta \simeq B_r \simeq \frac{2\pi}{c} I_\varphi.$$

$$\frac{dp}{dz} \simeq \frac{\varrho GM}{r^2} \frac{z}{r}; \qquad h \simeq \left(\frac{r^3}{GM} \frac{p}{\varrho}\right)^{1/2}.$$

$$F = \frac{GM\dot{M}}{4\pi r^3} \left[1 + \frac{1}{2}\left(\frac{r}{R}\right)^{3/2}\right]. \qquad 2F \simeq \frac{I_\varphi^2}{2h\sigma},$$

$$cCT^4 \simeq \kappa \Sigma F, \qquad 2F = \Sigma(\varepsilon_{ff} + \varepsilon_R),$$

Turbulent electrical conductivity, analog of alpha viscosity

$$\sigma_t = \frac{c^2}{\tilde{\alpha} 4\pi h \sqrt{P/\varrho}},$$

$$L \simeq \tfrac{1}{2}\dot{M}c^2 \simeq 5 \times 10^{31}\, m^2 \xi$$

$$\xi = \left(\frac{\varrho_\infty}{10^{-14}\ \mathrm{g\ cm^{-3}}}\right)\left(\frac{T_\infty}{10^4\ \mathrm{K}}\right)^{3/2}$$

$$B = 10^9\ \mathrm{Gs}\ m^{-1/2} x^{3/4} \alpha^{-1/2},$$

A hot corona around a black-hole accretion disk as a model for Cygnus X-1

G. S. Bisnovatyi-Kogan and S. I. Blinnikov

Institute for Space Research, USSR Academy of Sciences, Moscow

(Submitted April 15, 1976) Sov.Astron.Lett. 2, 191-193 (Sep.-Oct. 1976)

Another mechanism for producing fast particles is analogous to the pulsar process. If magnetized matter with low angular momentum falls into the black hole (in addition to the disk accretion), a strong poloidal magnetic field will arise [19]. By analogy to pulsars [20], rotation will generate an electric field of strength $E \approx -(v/c)B$ in which electrons are accelerated to energies Energy $\approx R(v/c)B\ e \approx 3 \cdot 10^4$ [B/(10^7 Gauss)] Mev where $v/c \approx 0.1$ and $R \approx 10^7$ cm is the characteristic scale. In a field $B \approx 10^7$ Gauss, such electrons will generate synchrotron radiation with energies up to $\approx 10^5$ keV. Just as in pulsars, it would be possible here for e^+e^- pairs to be formed and to participate in the synchrotron radiation.

Dynamo model of double radio sources

Lovelace, R. V. E.

Nature, vol. 262, Aug. 19, 1976, p. 649-652.

Jet formation in the accretion disk around BH (sketch)

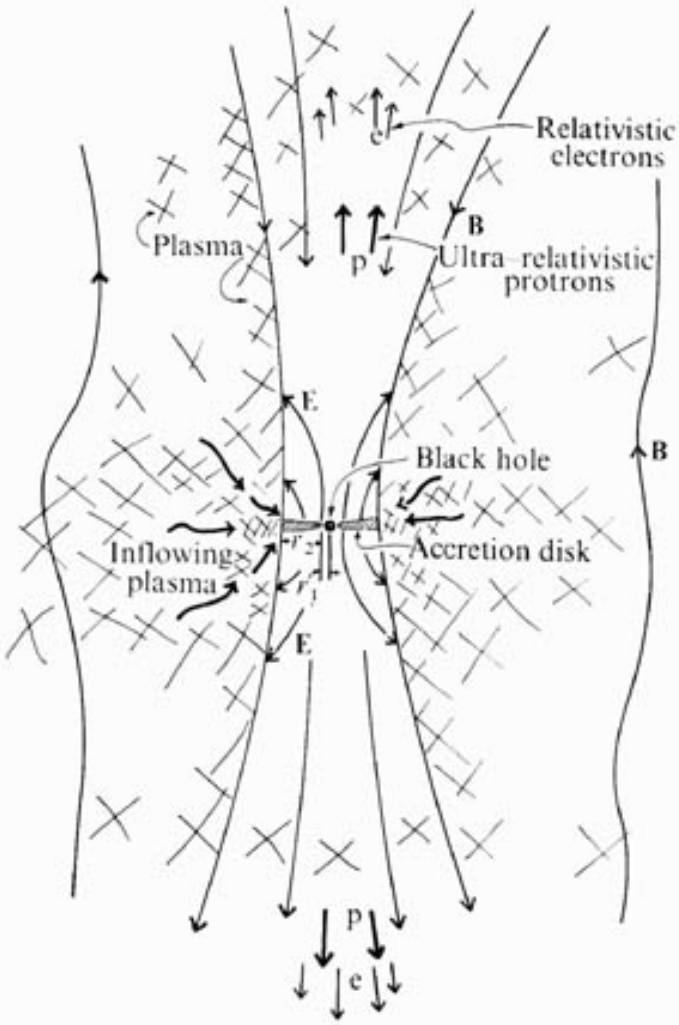

Sketch of picture of a disk accretion on to a black hole at sub-critical luminosity.

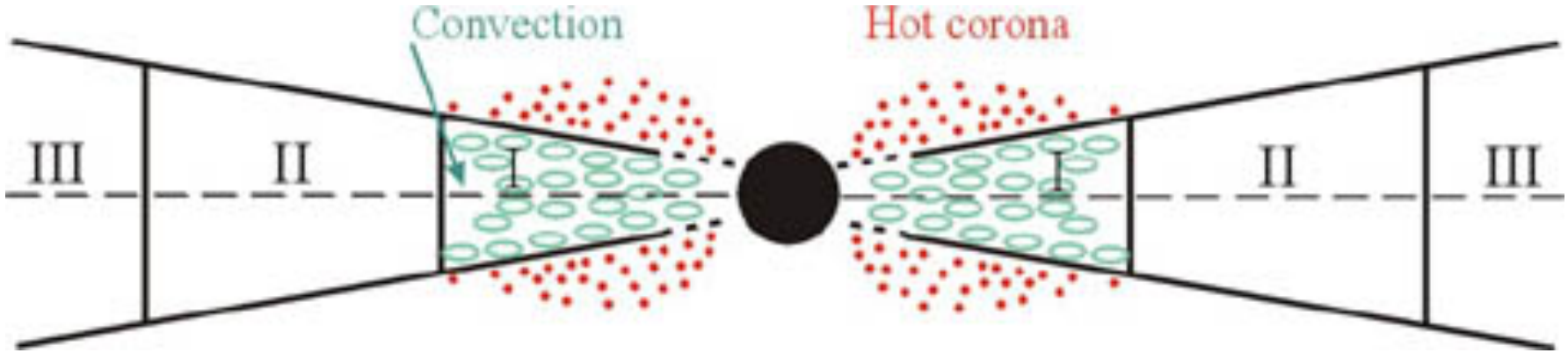

I – radiation dominated region, electron scattering.
II – gas-dominated region, electron scattering.
III- gas-dominated region, Krammers opacity.

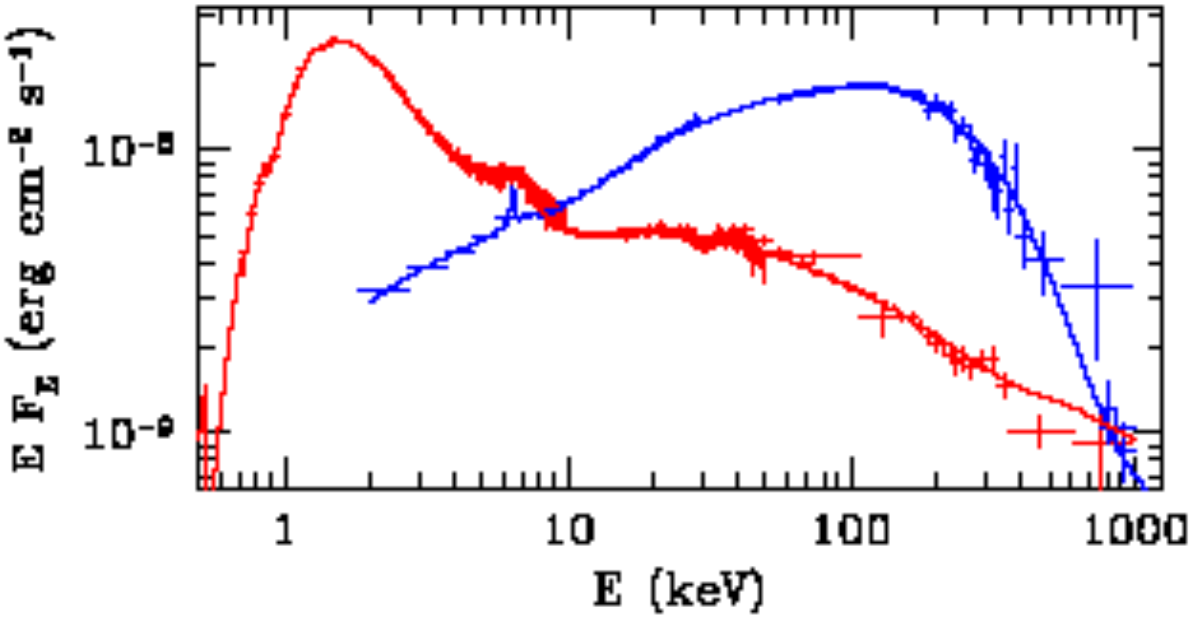

X-ray spectral states in Cyg X-1. Classical soft (red) and hard (blue) States, from Gierli´nski et al. (1999).

“alpha disk” model

Algebraic relation
(Shakura 1972)

$$t_{\phi r} = \alpha P$$

$t_{\phi r}$ – viscous stress

P – pressure

Angular velocity gradient dependent viscous stress

$$t_{\phi r} = \rho \nu r \frac{d\Omega}{dr}, \qquad \nu = \alpha \rho u_{s0} z_0$$

ν – kinematic viscosity coefficient

ρ – density

Ω – angular velocity

Two families of solutions to the steady state disk structure equations, for given alpha, $\dot{M}$

1. Optically thick ($\tau_* >> 1$) – unstable in the radiation dominated region with vertical radiative transfer

Emission of AGN in the UV - soft X-ray range

($T \sim 10^5$ K)

Emission of stellar BHs in the X-ray range

($T \sim 10^7$ K)

2. Optically thin ($\tau_* << 1$) - globally unstable

Hard X-ray and γ-ray emission of AGN and stellar BHs

($T \sim 10^9$ K)

Radiative flux from the disk surface

Optically thick limit ($\tau_* >> 1, \tau_0 >> 1$)

$F_0 = 2\, a\, T_c^4 c / 3\, \tau_0$

Optically thin limit ($\tau_* << 1, \tau_0 >> \tau_*$)

$F_0 = a\, T_c c\, \tau_\alpha$

τ_0 – total optical depth to electron scattering

τ_α - total optical depth to absorption

τ_* – effective optical depth, $\tau_* = (\tau_0\, \tau_\alpha)^{1/2}$

Solutions without advection

(BH mass = 10 solar masses, α=0.5) $r_* = r/r_g$, $r_g = GM/c^2$

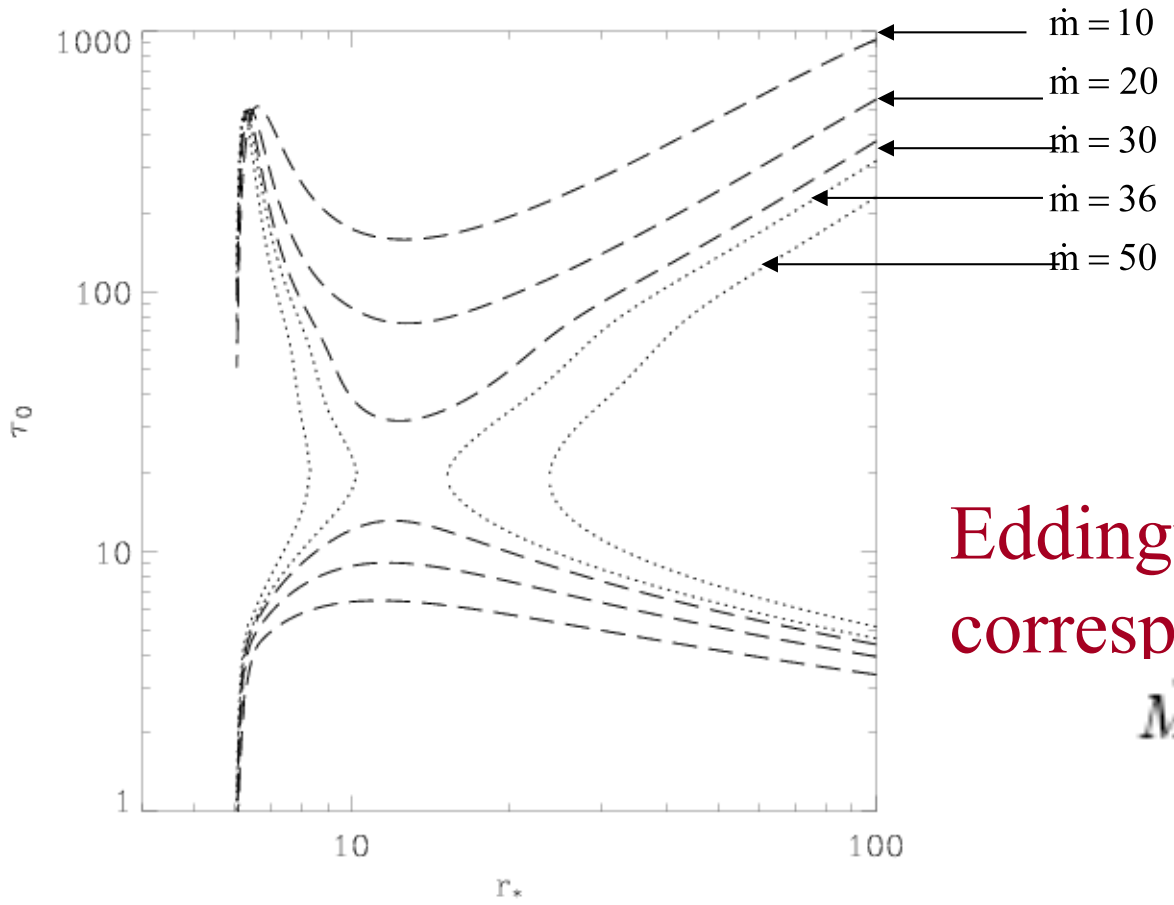

Eddington limit corresponds to $\dot{M} = 16$

The dependence of the Thomson scattering depth on the radius

Taking advection into account

The vertically averaged energy conservation

Paczynski. Bisnovatyi-Kogan (1981)

$Q_{adv}=Q^{+} - Q^{-},$ $\qquad Q_{\rm adv} = -\frac{\dot{M}}{2\pi r} T \frac{dS}{dr}$

The equation of motion in radial direction

$$v\frac{dv}{dr} = -\frac{1}{\rho}\frac{dP}{dr} + \left(\Omega^2 - \Omega_K^2\right) r$$

Set of equations for “αP” viscosity prescription with advection

$$\begin{cases} r\dfrac{v'}{v} = \dfrac{N}{D} \\ r\dfrac{c_s'}{c_s} = \left(1-\dfrac{v^2}{c^2}\right)\dfrac{N}{D} + 1 - r\dfrac{\Omega_K'}{\Omega_K} + \dfrac{\Omega^2-\Omega_K^2}{c_s^2}r^2 \\ \Omega = \dfrac{l_{in}}{r^2} + \alpha\dfrac{c_s^2}{vr} \end{cases}$$

where $()' \equiv \dfrac{d}{dr}$

N, D - functions of $r, \Omega, \Omega_K, \beta, v, c_s, l_{in}, \alpha, \dot{M}$

$$\beta = \frac{P_g}{P}, \quad (1-\beta)P = \frac{aT_c^4}{3}\frac{1+\dfrac{4}{3\tau_0}}{1+\dfrac{4}{3\tau_0}+\dfrac{2}{3\tau_*^2}}$$

$$T = \beta\frac{c_s^2 c^2}{R}$$

Artemova Yu. V.
Bisnovatyi-Kogan G. S.
Igumenshchev I. V.
Novikov I. D.
ApJ, 2006, 637:968–977

Boundary conditions

$r >> 100\ r_g \quad \rightarrow \quad$ ” Standard disk ”

Parameters in singular point must satisfy conditions

$$N = 0$$

$$D = 0$$

The behavior of the integral curves in presence of singular points

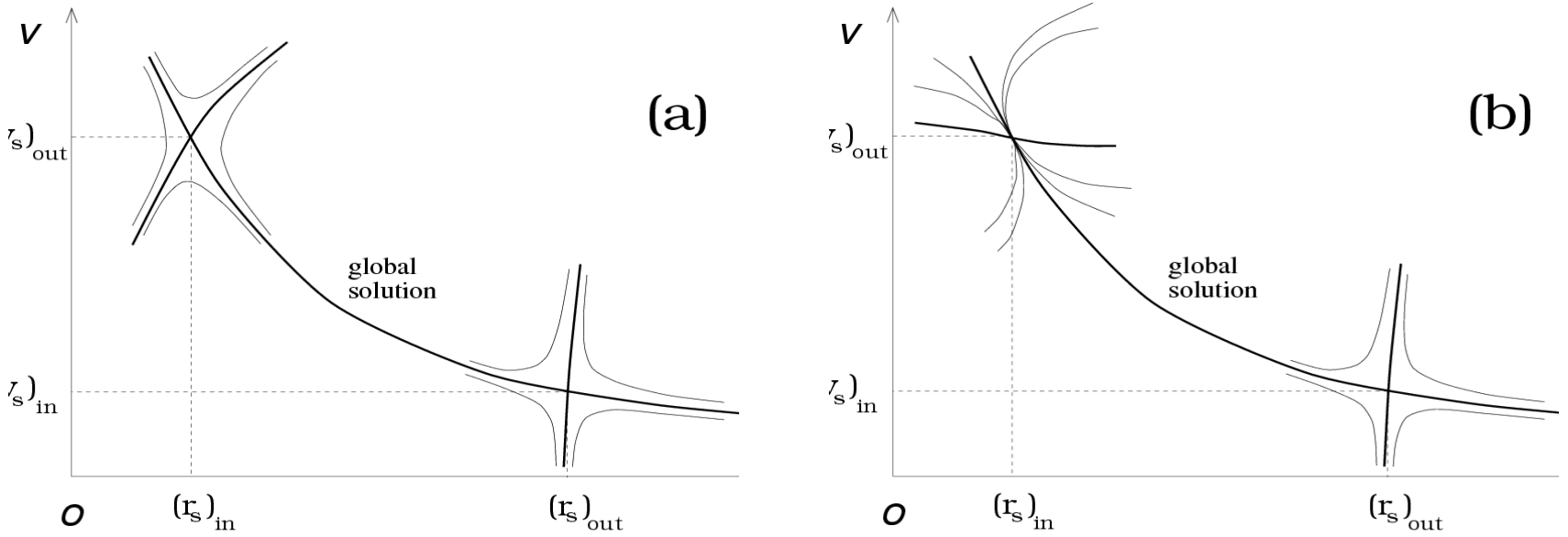

Outer singular point is a non-important artefact

Solutions with advection
(BH mass = 10 solar masses, α=0.5)

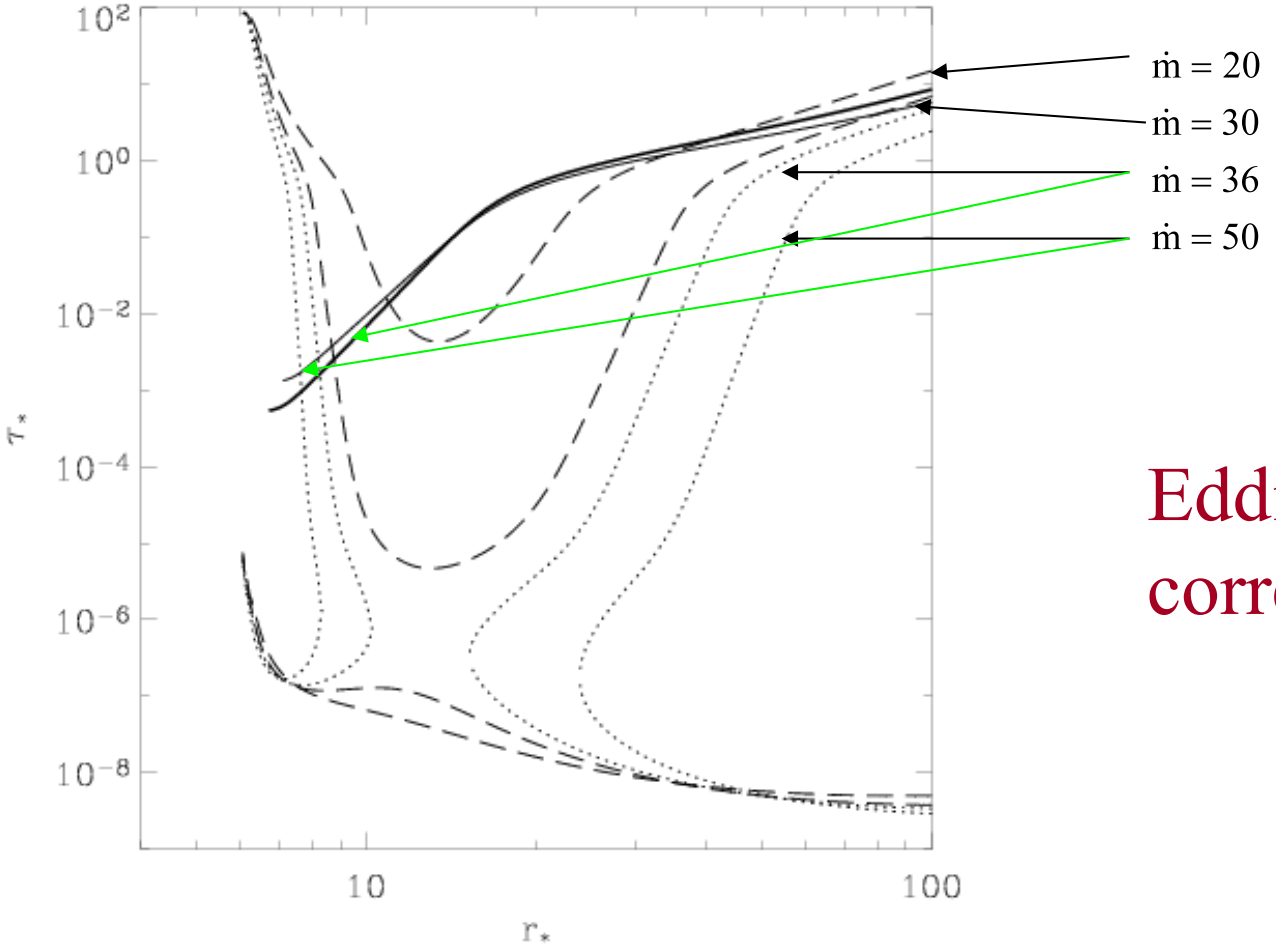

Eddington limit corresponds to $\dot{M} = 16$

The dependence of the effective optical depth on the radius

Solutions with advection

(BH mass = 10 solar masses, α=0.5, accretion rate = 48.0)

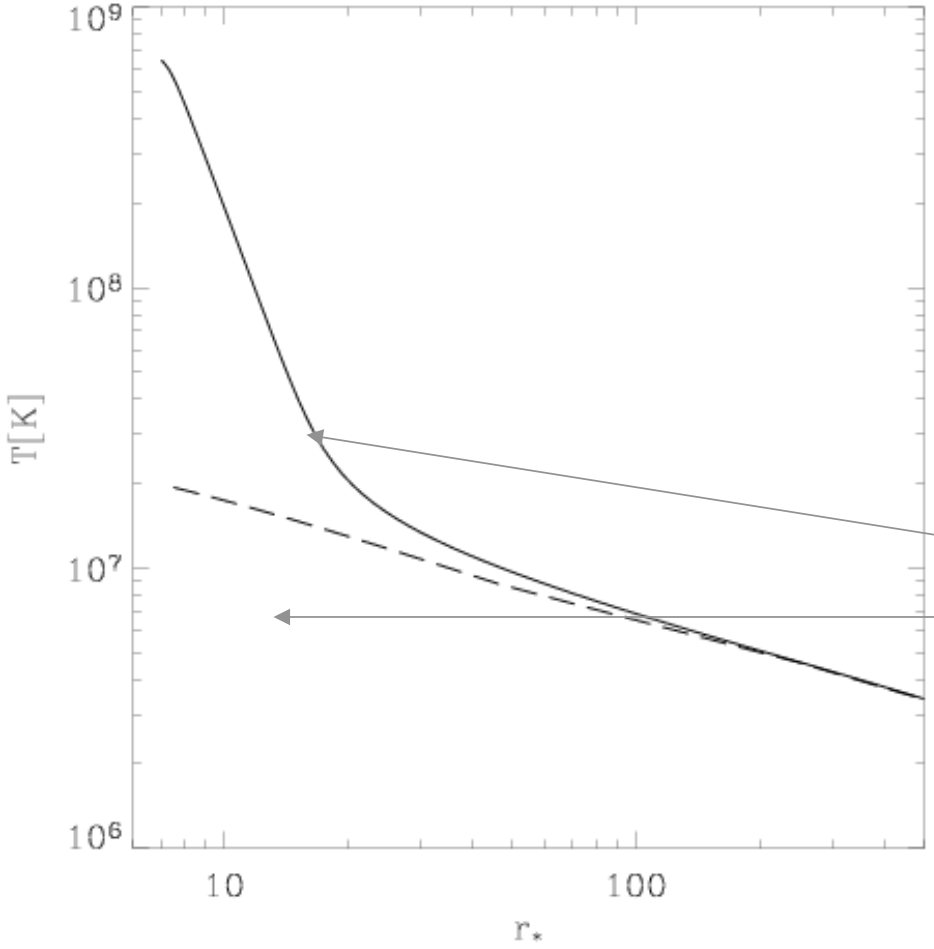

Artemova, Bisnovatyi-Kogan, Igumenshchev , Novikov,

ApJ, 2006, 637, 968

With optical depth transition

Without optical depth transition

The dependence of the temperature on the radius

A.S. Klepnev and G. S. Bisnovatyi-Kogan

Astrophysics, Vol. 53, No. 3, p. 409-418, 2010

$$\tau_* = [(\tau_0 + \tau_\alpha)\ \tau_\alpha]^{1/2}$$

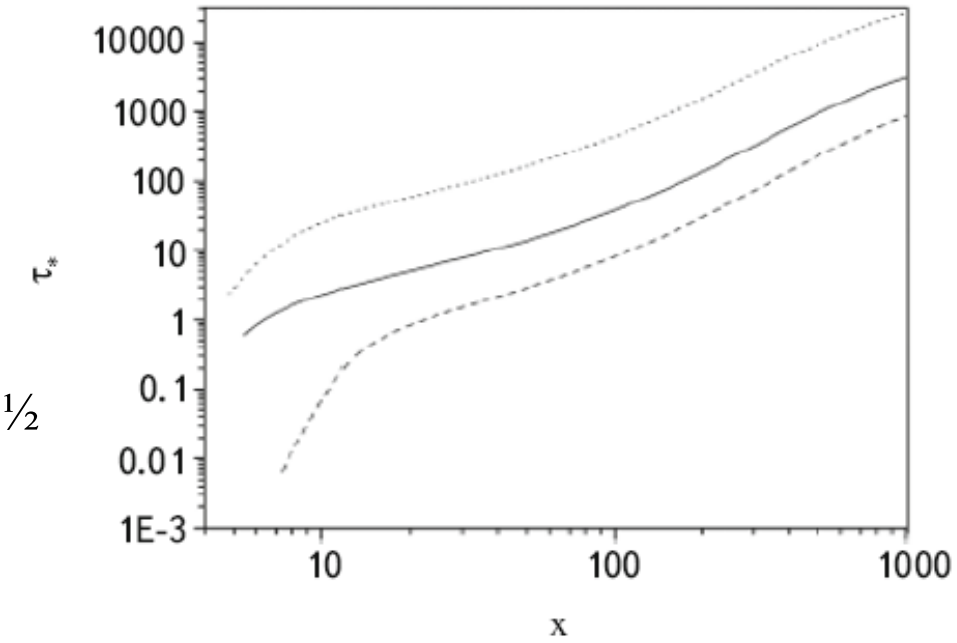

Fig. 2. The radial dependence of the effective optical depth of the accretion disk for an accretion rate $\dot{m} = 50$ and viscosity parameters $\alpha = 0.01$ (dotted curve), $\alpha = 0.1$ (smooth curve), and $\alpha = 0.4$ (dashed curve).

A.S. Klepnev and G. S. Bisnovatyi-Kogan

Astrophysics, Vol. 53, No. 3, p. 409-418, 2010

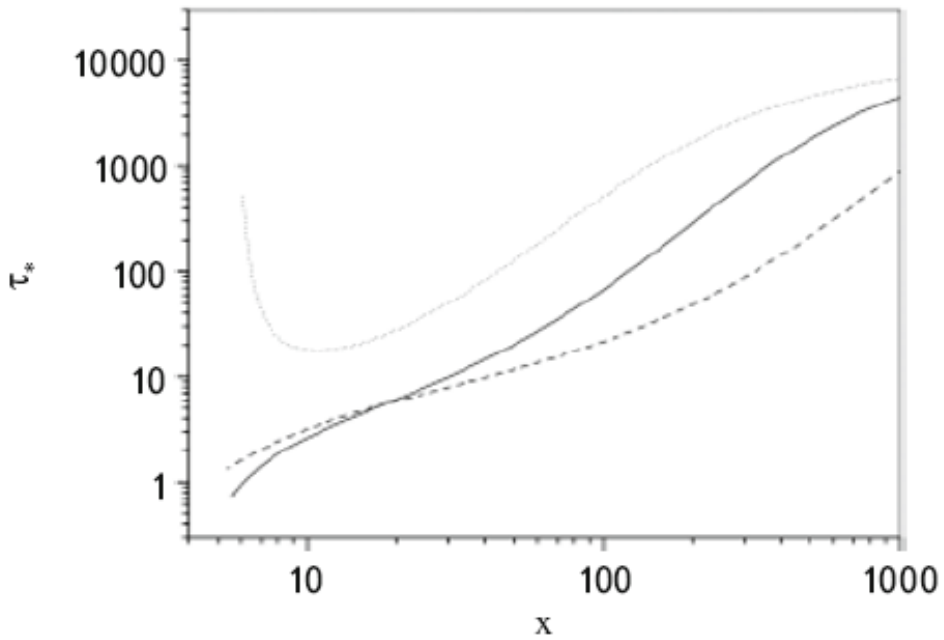

Fig. 4. The radial dependence of the effective optical depth τ_e of the accretion disk for accretion rates $\dot{m} = 8$ (dotted curve), $\dot{m} = 30$ (smooth curve), and $\dot{m} = 150$ (dashed curve), and a viscosity parameter $\alpha = 0.1$.

A.S. Klepnev and G. S. Bisnovatyi-Kogan

Astrophysics, Vol. 53, No. 3, p. 409-418, 2010

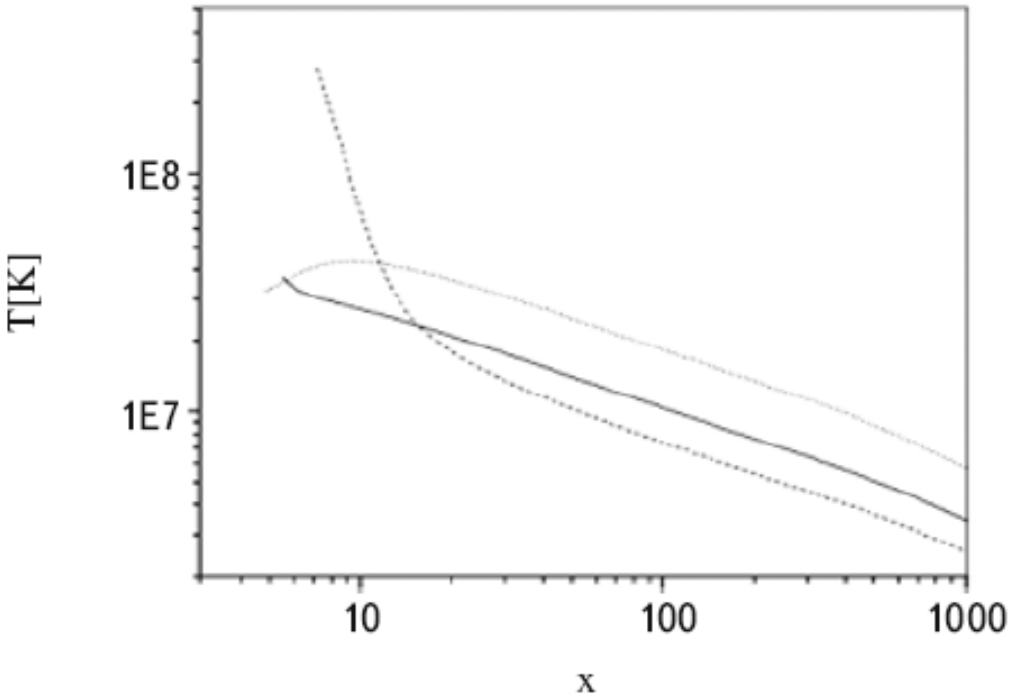

Fig. 3. The radial dependence of the temperature of the accretion disk for an accretion rate $\dot{m} = 50$ and viscosity parameters $\alpha = 0.01$ (dotted curve), $\alpha = 0.1$ (smooth curve), and $\alpha = 0.4$ (dashed curve).

In Kerr metric BH the temperature in the optically thin region exceeds 500 keV – pair creation

Mon. Not. R. Astron. Soc. **267**, 235–240 (1994)

Magnetic field dragging in accretion discs

S. H. Lubow,[1,2]★ J. C. B. Papaloizou[1] and J. E. Pringle[1,2]

We consider a thin accretion disc of half-thickness H, vertically threaded by a magnetic field. The field is due to contributions from both the disc current and an external current (giving rise to a uniform external field). We derive an integro-differential equation for the evolution of the magnetic field, subject to magnetic diffusivity η and disc accretion with radial velocity v_r. The evolution equation is solved numerically, and a steady state is reached. The evolution equation depends upon a single, dimensionless parameter $\mathscr{D} = 2\eta/(3H|v_r|) = (R/H)(\eta/\nu)$, where the latter equality holds for a viscous disc having viscosity ν. At the disc surface, field lines are bent by angle i from the vertical, such that $\tan i = 1.52\mathscr{D}^{-1}$. For values of $\mathscr{D}$ somewhat less than unity, the field is strongly concentrated towards the disc centre, because the field lines are dragged substantially inwards.

Magnetic diffusivity is of the order of kinematic viscosity in the turbulent disk, **D>>1**

$$\sigma_t = \frac{c^2}{\tilde{\alpha} 4\pi h \sqrt{P/\varrho}},$$

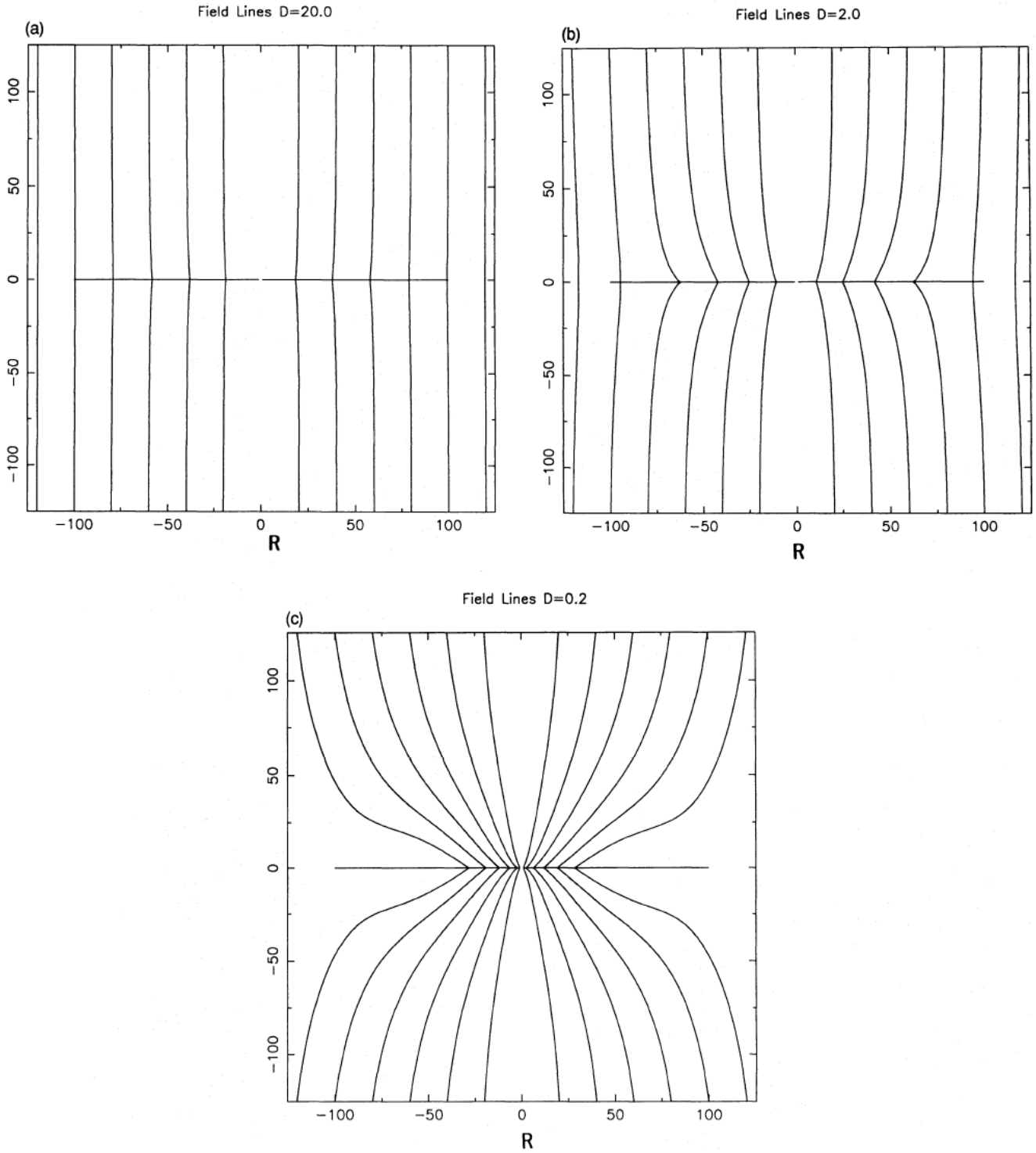

Figure 2. Plot of field lines in the equilibrium disc for the three values of $\mathscr{D}$ in Fig. 1. In each plot, the horizontal line marks the horizontal region occupied by the disc.

Large scale magnetic field is amplified during the disk accretion, due to currents in the radiative outer layers, with very high electrical conductivity

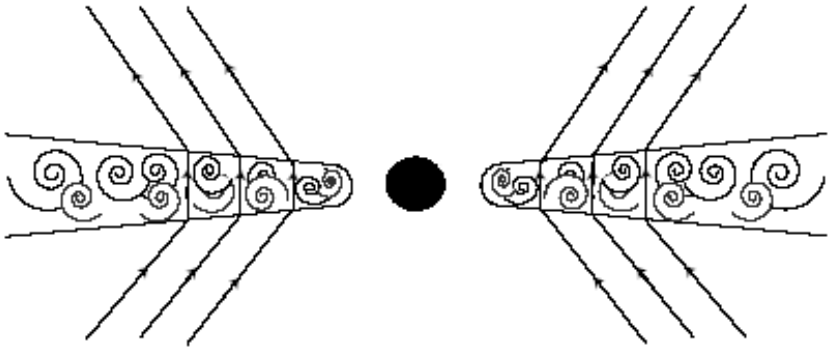

Figure 2: Sketch of the large-scale poloidal magnetic field threading a rotating turbulent accretion disk with a radiative outer boundary layer. The toroidal current flows mainly in the highly conductive radiative layers. The large-scale (average) field in the turbulent region is almost vertical.

Bisnovatyi-Kogan, Lovelace, 2007, ApJL, **667**: L167–L169, 2007 October 1

In this situation we may expect a nonuniform distribution of the angular velocity over the disk thickness: The main body of the turbulent disk is rotates with the velocity close to the Keplerian one, and outer optically thin layers rotate substantially slower by ~ 30%.

Turbulence in the outer layers is produced by shear instability

$\kappa_{es}\Sigma_{ph} = 2/3\ ,$ $\Sigma_{ph} = 5/3\ (\mathrm{g/cm^2})$ for the opacity of the Thomson scattering

$$\Sigma_d = \frac{80\sqrt{2}}{9\alpha}\frac{x^{3/2}}{\dot{m}}\left(1-\sqrt{\frac{3}{x}}\right)^{-1}$$

$$B_z \sim \sqrt{\Sigma_{ph}}.$$

B(min) ~ 10^8/sqrt(M_solar) for Schwarzschild BH

$$\dot{m} = \frac{\dot{M}c^2}{L_c}\ , \qquad L_c = \frac{4\pi cGM}{\kappa_{es}}$$

Magnetic field may be ~10 times larger for rapid Kerr BH

ADVECTION/DIFFUSION OF LARGE-SCALE B FIELD IN ACCRETION DISKS

R.V. E. Lovelace, D.M. Rothstein, & G.S. Bisnovatyi-Kogan

ApJ, **701**:885–890, 2009 August 20

Here, we calculate the vertical (z) profiles of the stationary accretion flows (with radial and azimuthal components), and the profiles of the large-scale, magnetic field taking into account the turbulent viscosity and diffusivity due to the MRI and the fact that the turbulence vanishes at the surface of the disk.

Advection/Diffusion of B Field in Disks, G. S. Bisnovatyi-Kogan & R.V.E. Lovelace, ApJ, **748** (2012)

Main Equations

$$\rho \frac{d\mathbf{v}}{dt} = -\nabla p + \rho \mathbf{g} + \frac{1}{c}\mathbf{J} \times \mathbf{B} + \mathbf{F}^{\nu} \ ,$$

$$\frac{\partial \mathbf{B}}{\partial t} = \nabla \times (\mathbf{v} \times \mathbf{B}) - \nabla \times (\eta \nabla \times \mathbf{B}) \ .$$

$$\nu = \mathcal{P} \ \eta = \alpha \ \frac{c_{s0}^2}{\Omega_K} \ g(z) \ ,$$

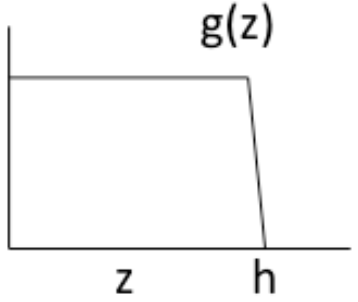

Equations:

stationary axisymmetric accretion flows, and the weak large-scale magnetic field, taking into account the turbulent viscosity and diffusivity

$[v_r(z),\, v_\phi(z),\, v_z = 0]$ $\qquad$ $[B_r(z),\, B_\phi(z),\, B_z \approx \text{const}]$.

$$\alpha^4\beta^2\frac{\partial^2}{\partial\zeta^2}\left(g\frac{\partial}{\partial\zeta}\left(\tilde{\rho}g\frac{\partial}{\partial\zeta}\left(\frac{1}{\tilde{\rho}}\frac{\partial}{\partial\zeta}\left(\tilde{\rho}g\frac{\partial u_r}{\partial\zeta}\right)\right)\right)\right)$$
$$-\alpha^2\beta\mathcal{P}\frac{\partial^2}{\partial\zeta^2}\left(g\frac{\partial}{\partial\zeta}\left(\tilde{\rho}g\frac{\partial}{\partial\zeta}\left(\frac{u_r}{\tilde{\rho}g}\right)\right)\right)$$
$$-\alpha^2\beta\mathcal{P}\frac{\partial^2}{\partial\zeta^2}\left(\frac{1}{\tilde{\rho}}\frac{\partial}{\partial\zeta}\left(\tilde{\rho}g\frac{\partial u_r}{\partial\zeta}\right)\right)$$
$$+\alpha^2\beta^2\frac{\partial^2}{\partial\zeta^2}(\tilde{\rho}g(u_r - gu_0)) + \mathcal{P}^2\frac{\partial^2}{\partial\zeta^2}\left(\frac{u_r}{\tilde{\rho}g}\right)$$
$$+3\beta\mathcal{P}^2\frac{u_r}{g} = 0.$$

$$\nu = \mathcal{P}\eta = \alpha\frac{c_{s0}^2}{\Omega_K}g(z),$$

$$g(\zeta) = \left(1 - \frac{\zeta^2}{\zeta_S^2}\right) \quad ,$$

$$\delta \ll 1.$$

$$u_\phi = 1 + \delta u_\phi \quad , \quad \delta u_\phi = -\frac{k_p\varepsilon^2}{2} - \frac{\varepsilon\mathcal{P}u_r}{2\beta\tilde{\rho}g} + \frac{\alpha^2\varepsilon}{2\tilde{\rho}}\frac{\partial}{\partial\zeta}\left(\tilde{\rho}g\frac{\partial u_r}{\partial\zeta}\right)$$

Boundary condition on the disk surface: $\left.\frac{\partial u_r}{\partial\zeta}\right|_{\zeta_S-} = 0$.

G.S. Bisnovatyi-Kogan, R.V. E. Lovelace (2011)

1. **Boundary condition on the disk surface: u_r=0**

2. **Only one free parameter: Magnetic Prandtl number =\nu_t/\eta~1**

In a stationary disk vertical magnetic field has a unique value

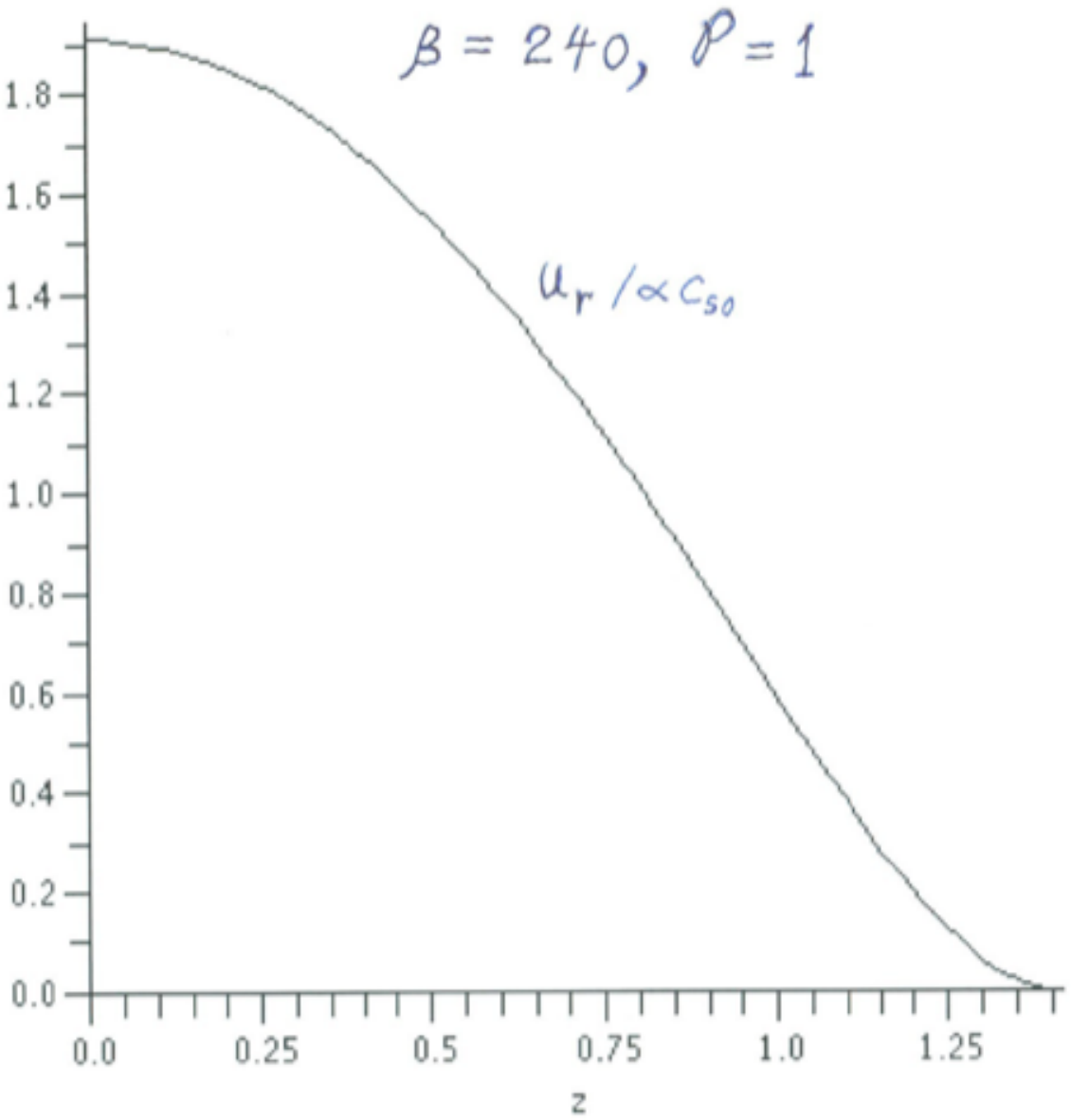
β = 240, β = 1
$u_r / \propto c_{s0}$
1.8
1.6
1.4
1.2
1.0
0.8
0.6
0.4
0.2
0.0
0.0
0.25
0.5
0.75
1.0
1.25
z

Jet in M 87:

Radio: 6 cm (up
Optical: V-band
(middle),
Chandra:
X-ray 0.1-10 keV
(down)

Wilson , Yang
(2001)

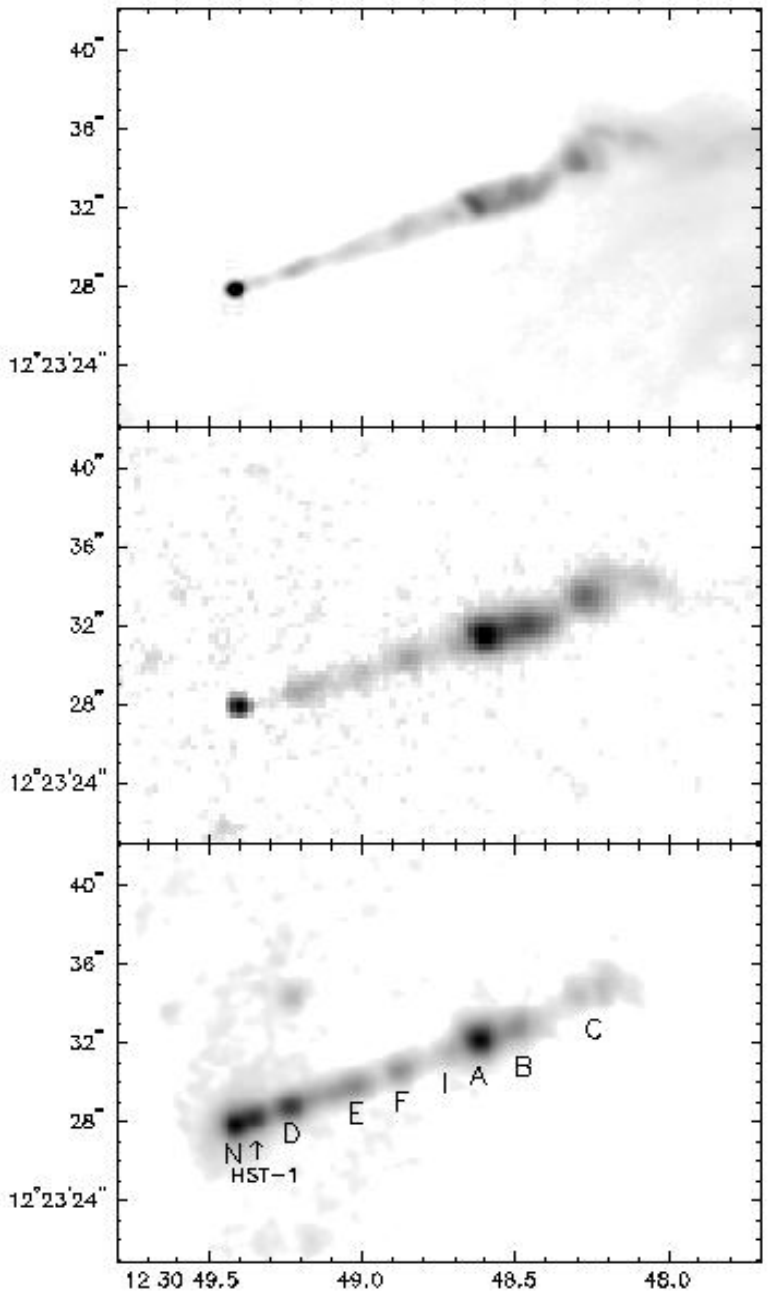

W.A.Hiltner
ApJ, 1959

PHOTOELECTRIC POLARIZATION OBSERVATIONS OF THE JET IN M87*

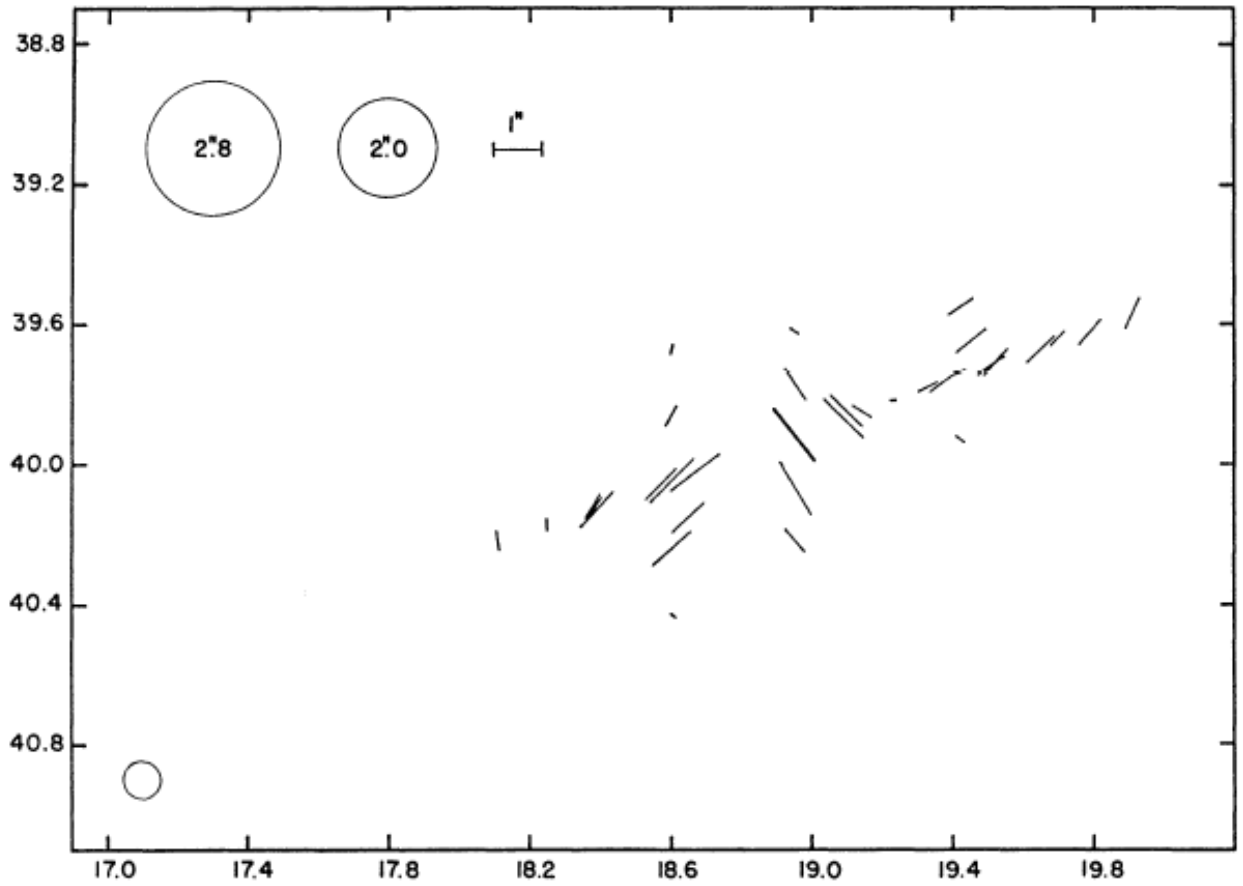

FIG. 1.—Polarization observations of M87. The co-ordinates refer to the observed position relative to a guide star. All lines refer to individual observations except the heavy one, which is the mean of ten observations. The relative sizes of the diaphragms used are shown in the upper left of the figure. The position of the nucleus of M87 is shown by a small open circle in the lower left.

Magnetic collimation is connected with torsional oscillations of a cylinder with elongated magnetic field.

We consider a cylinder with a periodically distributed initial rotation around the cylinder axis.

The stabilizing azimuthal magnetic field is created by torsional oscillations.

Approximate simplified model is developed. Ordinary differential equation is derived, and solved numerically, what gives a possibility to estimate quantitatively the range of parameters where jets may be stabilized by torsional oscillations.

Bisnovatyi-Kogan, MNRAS 376, 457 (2007)

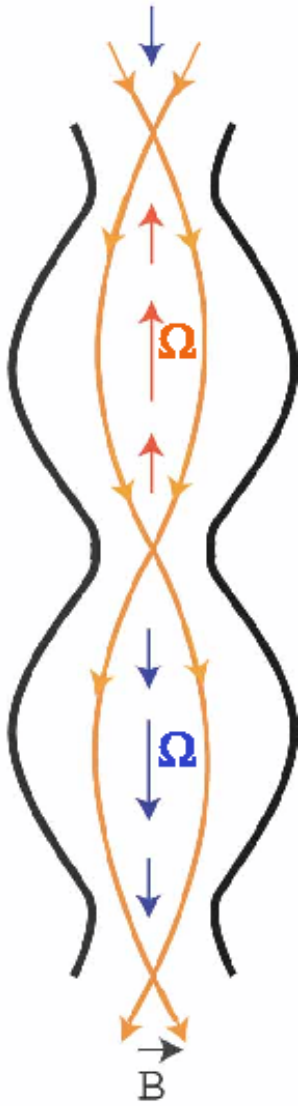
Ω
Ω
B

Three possibilities

1. The oscillation amplitude is low, so the cylinder suffers unlimited expansion (no confinement)

2. The oscillation amplitude is too high, so the pinch action of the toroidal fieeld destroys the cylinder, and leads to formation of separated blobs.

3. The oscillation amplitude is moderate, so the cylinder survives for an unlimited time, and its parameters (radius, density, magnetic field etc.) change periodically, quasi-periodically, or chaotically in time.

Jet formation in MRE. Dipole-like initial magnetic field

S. G. Moiseenko, G. S. Bisnovatyi-Kogan and N. V. Ardeljan

Mon. Not. R. Astron. Soc. **370,** 501–512 (2006)

A magnetorotational core-collapse model with jets

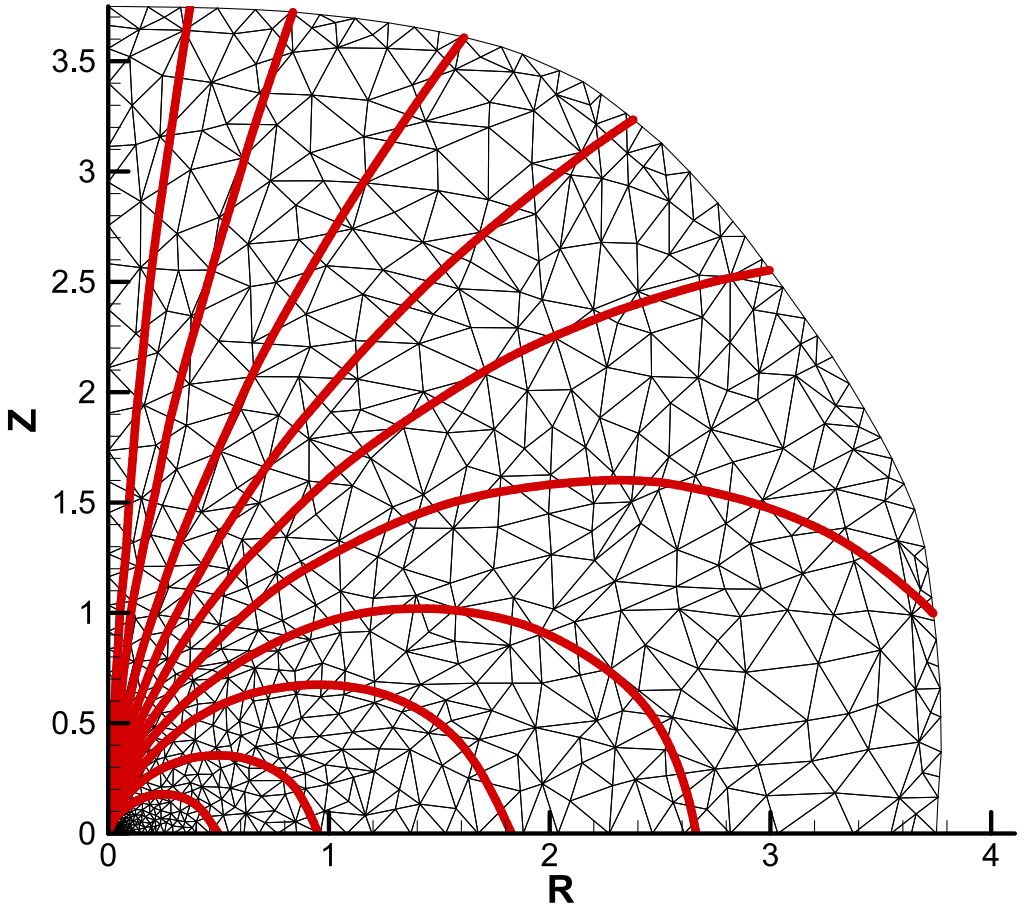

Jet formation in MRE:

velocity_field evolution

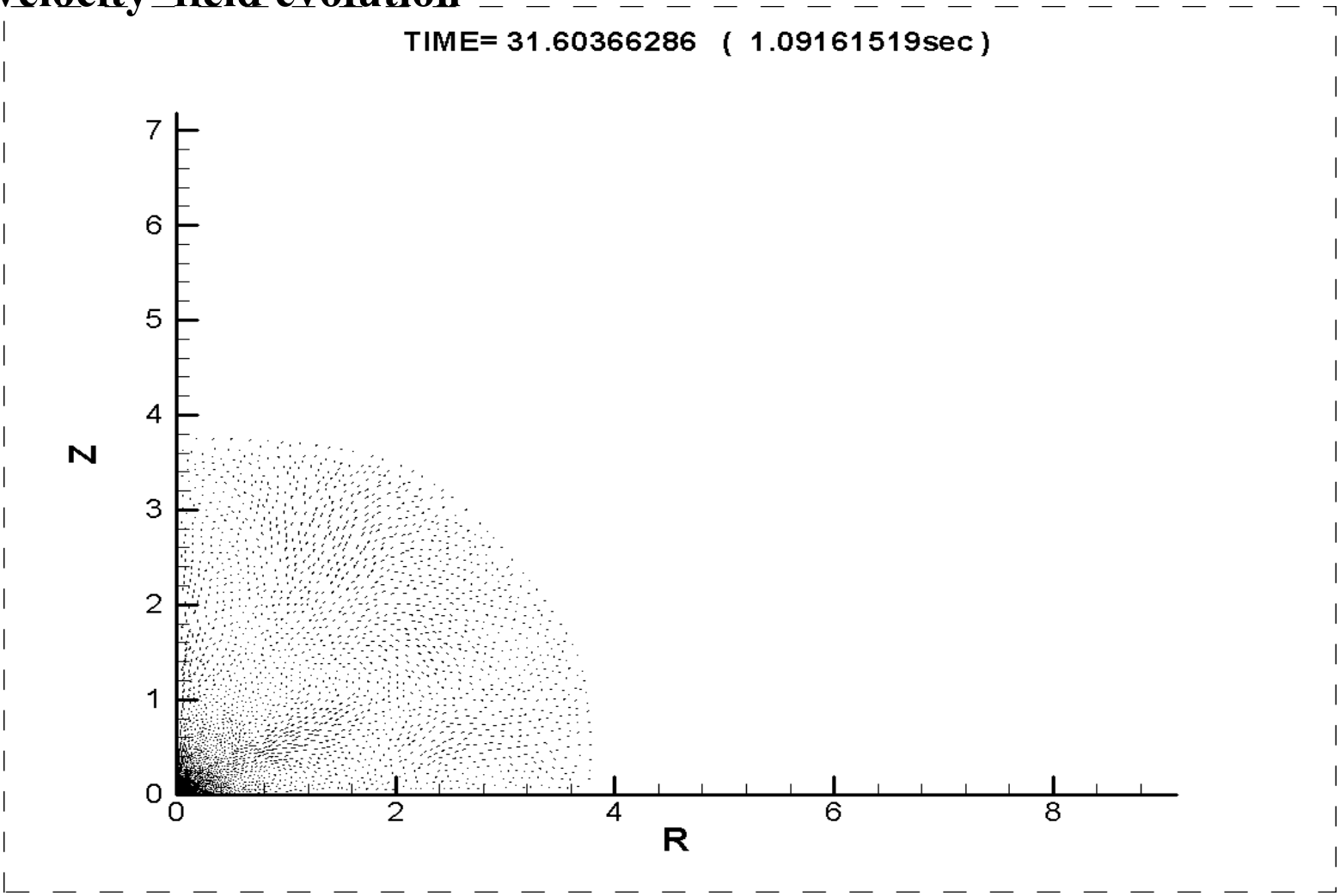

Conclusons

1. Global, trans-sonic solution exists, which at high *m* and *α*, is characterized by a continuous transition of the disk from optically thick in the outer region to optically thin in the inner region.

2. The model, with a correct accounting for the transition between the optically thick and optically thin regions, reveals the existence of a temperature peak in the inner (optically thin) region. This peak might cause the appearance of a hard component in the spectrum, which could be observed. A high temperature in the inner region of an accretion disk may lead to the formation of electron-positron pairs and change the emission spectrum of the disk at energies of 500 keV and above (in Kerr metric).

4. When α = 0.5, a very substantial optically thin region is observed, when α = 0.1 we have a slight optically thin region, and when α = 0.01 no optically thin region is seen at all.

5. This field is amplified during disk accretion due to high conductivity in outer radiative layers. Stationary solution corresponds to \beta=240 for Pr=1.

6. Jets from accretion disk are magnetically collimated by large scale poloidal magnetic field by torsion oscillations, which may be regular or chaotic. Jets may be produced in magneto-rotational explosions (supernova etc.)